Supporting Information

Early detection of amyloidopathy in Alzheimer's mice by hyperspectral endoscopy.

Swati S. More[1], James Beach[2], Robert Vince[1*]

[1]Center for Drug Design, Academic Health Center, University of Minnesota, Minneapolis, MN 55455; and [2]CytoViva Inc., Auburn, Alabama

*Corresponding author:

Professor Robert Vince, Center for Drug Design, 308 Harvard Street SE, 8-123A WDH, Minneapolis, MN 55455, USA. Phone: 612-624-9911; Fax: 612-626-2633; E-mail: vince001@umn.edu.

I. In-vivo light absorption spectrum of RPE melanin

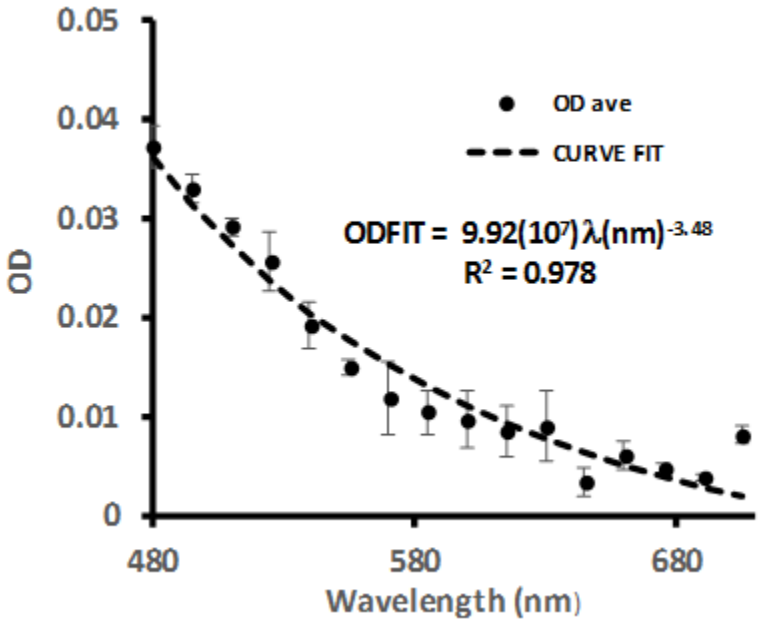

Figure S1. Melanin absorption spectrum from TEFI spectral recording. Melanin's light absorption spectrum was extracted using the form of equation 1 (Methods Section) from pairs of measurements (N=3) taken from the TEFI image of the WT retina (570 nm). In each pair one measurement site was a darkly pigmented area of retina, yielding reflected value I_{dark} while the other site appeared relatively lighter, yielding I_{light}. The spectral curve was then found as:

$$OD_{melanin} = Log_{10}(I_{light} / I_{dark})$$

This shows that our spectral imaging system was sensitive to melanin light absorption as well as hemoglobin absorption.

II. TEFI image of fundus of a white mouse using 570 nm illumination

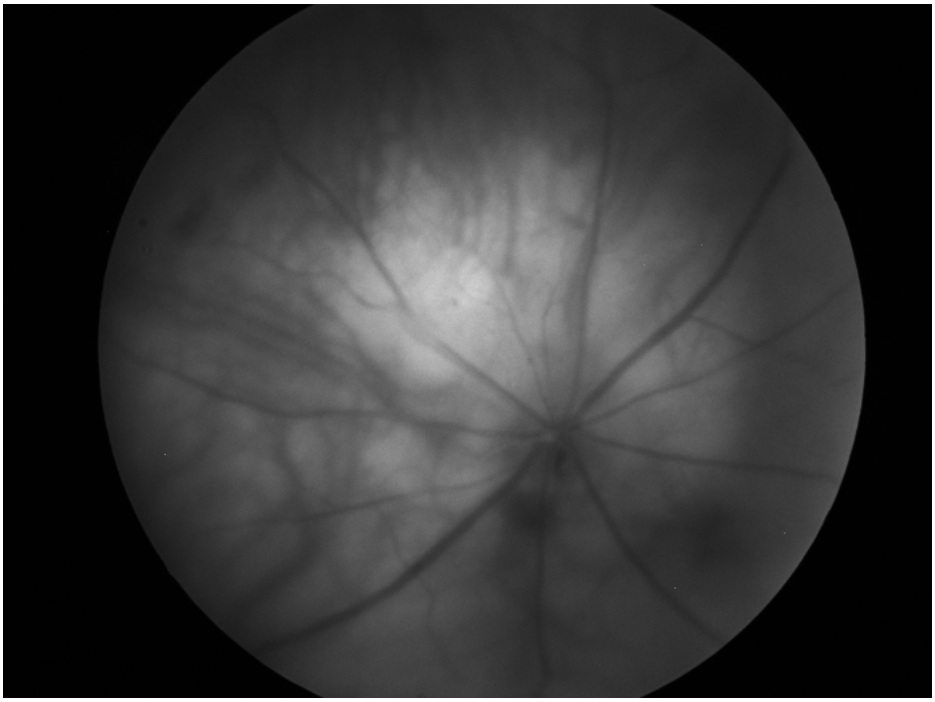

Figure S2. A representative monochromatic image from a white mouse retina. Detailed visualization of arteries, veins, nerve fibers and choroidal capillaries was possible with optic nerve in the center. Brightness of the captured image was 2.5-3.0 fold higher than the aged-matched B6C3F1J mice.

III. Light diffusion in specimens of retina

Retinal whole mount

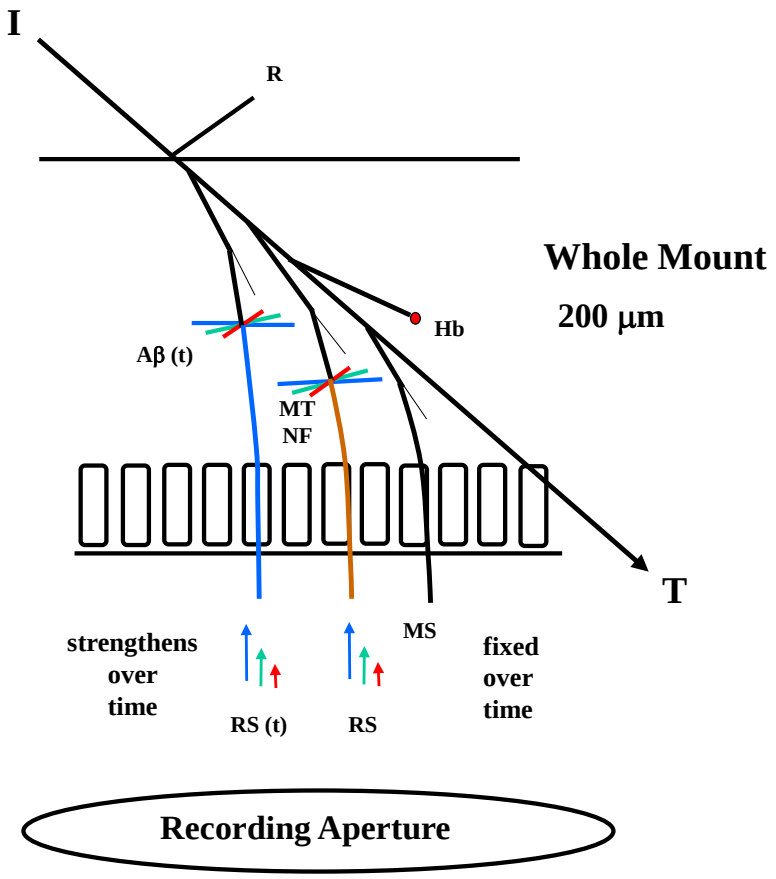

Figure S3. Light paths in retinal whole mount. In previously reported hyperspectral recordings from cells incubated with $A\beta^{1-42}$, and retinal wholemounts from Alzheimer's donors, we employed dark-field microscopy to record the scatter from light transmitted through the cell or retina. In comparison with unincubated cells and normal donor retina, the recorded spectrum showed reduced intensity at shorter wavelengths, similar to our finding between live WT and APP/PS1 mouse using reflected light. The similarity in results can be explained by considering tissue optical properties. In the dark field recordings the oblique angle of illumination was 60^{o} (NA = 1.3). A portion of the incident light penetrates the tissue. The light undergoes multiple forward scattering which directs a portion to the recording aperture. Rayleigh scattering will occur from neural structures (orange path) and, as we propose, from the accumulted beta-amyloid aggregation products (blue path). The side-directed light paths and reduction in

strength of exiting light are conveyed by colors representing changes in scattering efficiency over wavelength. A rise in the Rayleigh scatter, such as from a build-up of amyloid aggregation over time, will produce spectral changes in exiting light similar to those measured from the live mouse.

Live mouse retina

The ocular fundus, which supports the retina, is comprised of layers containing the neurosensory retina, photoreceptor layer, pigmented epithelium, choroidal blood supply and scleral backing. Light paths in these layers are dependent on tissue optical properties of each layer (Table S1).

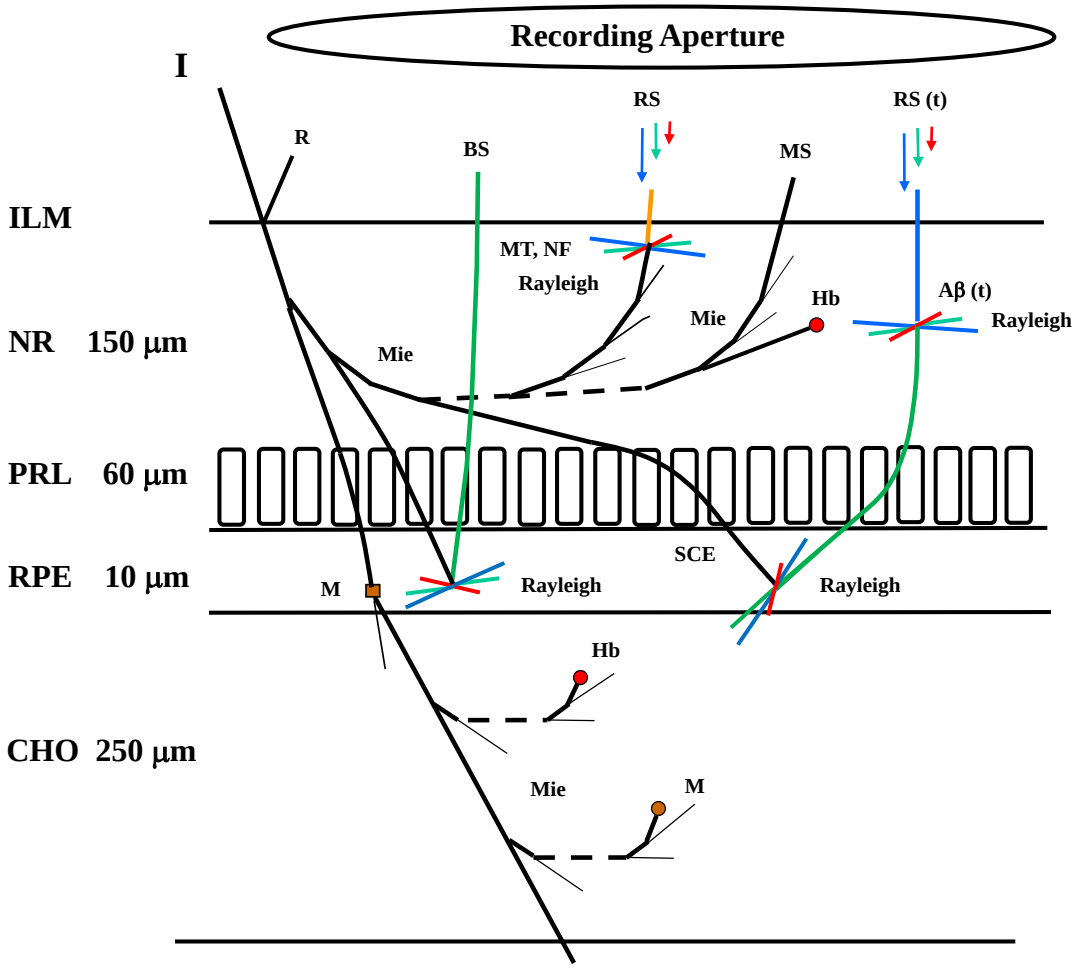

Figure S4. Pictorialized light paths through layers of the ocular fundus showing representative paths for Mie (dark lines) and Raleigh scattering (red, green and blue

lines), which ultimately yield an optical signal for the presence of amyloid aggregates in the neural retina (NR). Broad band light (I) from fiber optics surrounding one side of the endoscope (crescent illumination) enters the eye at a mean angle of 22° (see Fig. 1), passing through the pupil, lens and vitreous cavity to the inner limiting membrane (ILM), where approximately one-third is reflected (R). The remainder is transmitted into the neural retina and nerve fiber layer (NFL) on the retinal surface, and to deeper layers which include the retinal pigment epithelium (RPE) and choroid (CHO). RPE thickness in the diagram is enlarged for clarity. The RPE contains melanin granules (M) which produce strong absorption (brown circle in RPE layer). In the brown pigmented mouse the presence of large amounts of RPE melanin, along with absorption by choroidal hemoglobin and melanin (brown and red circles located in CHO layer), effectively limit the light reflux from deeper layers, so that light that has interacted with the choroidal layer makes a weak contribution to light returning from the retina. The RPE layer gives a reflection presumably by backscatter (Rayleigh scatter) from smaller granules or other tissue structures.[1,2] In our diagram this appears as back and side scatter (green light paths) within the RPE layer. The refection appears strong because this layer blocks light reflux from deeper layers.[3] Larger melanin granules (0.5 - 1.0 μm) scatter light mostly in the forward direction (Mie scatter, Brown Square in RPE). The RPE layer, being relatively thin and highly absorptive, does not return significant light to the NR though multiple scattering[4]. Greater thickness of the NR and CHO allows light diffusion to become isotropic in these layers, however absorption in the CHO limits return of light. Here we have schematized the diffusion by showing light paths from successive Mie forward scatter events over mean deflections (angled with respect to thin lines, see Table S1). Actual distances required for multiple forward scattering to return light are given in Table 1 (isotropic diffusion distance d_{isot}). Since light diffusion in the CHO is largely blocked from exiting the retina, the light we measure comes either from reflection at the ILM, backscatter off the RPE or multiple forward scatter within the NR. Because photoreceptors act as optical waveguides (Stiles-Crawford effect, SCE), light traversing the photoreceptor layer becomes more aligned with the receptors[3], increasing the amount of returned light. Light also interacts in the NR and NFL with small structures which include microtubules and neurofilaments (MT and NF symbols), creating side-

and back-directed light from single instances of isotropic Rayleigh scattering. For light paths leaving the retina, Rayleigh scatter reduces the intensity of measured light (orange path). In Alzheimer's disease the authors have proposed that, over time, additional Rayleigh scattering is caused by accumulation of soluble $A\beta^{1-42}$ aggregates (Aβ) in the neural retina, which leads to a further reduction in measured light (blue path). Light which is on an exit path within the recording aperture constitutes the portion of light that is measured. On this final path, Rayleigh scatter from small particles, some being normal components of the retina (MT and NF) and others involving amyloid-β aggregates (Aβ) will produce side- and back-directed light paths, reducing the measured light. As the beta-amyloid aggregation products accumulate over time, the effect of Rayleigh scatter is enhanced. Since Rayleigh scatter efficiency $\eta(\lambda)$ goes as the inverse fourth power of the wavelength, it produces a spectral change in the measured light, such that the measured light is reduced at shorter wavelengths. These effects are shown in color with arrows opposed to exit paths and side-directed light paths at scatter centers. The authors have proposed that these spectral changes caused by buildup of amyloid-β aggregates over time may be an early indicator for Alzheimer's disease.

Table S1. Optical properties influencing light paths in retinal layers for visible wavelengths

Layer	thickness (μm)	anisotropy (g)	mean deflection angle θ [#] (°)	scattering coefficient[+] μ_s (mm^{-1})	absorption coefficient[+] μ_a (mm^{-1})	mean free path[◊,×] μ_s^{-1} (μm)	isotropic diffusion[Δ,×] d_{isot} (μm)
neural retina	200 [5]	0.97 [2]	14	32 [2], 28 [6]	0.5 [2], 0.4 [6]	31 [2], 35 [6]	685 [2], 806 [6]
RPE	10 [2]	0.84 [2]	33	120 [2]	110 [2]	8.3	7.7
choroid	250 [2]	0.94 [2]	20	75 [2]	25 [2]	13	34

[+] value at 550 nm - reference 2; at 514 nm - reference 6

[×] calculated from the reported g, μ_a and μ_a.

[#] the mean cosine of deflection angles gives the anisotropy: $g = \langle\cos\theta\rangle$

[◊] mean free path length between Mie scatter events, given by $1/u_s$

[Δ] mean distance to achieve isotropic light diffusion from multiple forward scattering: $d_{isot} = (\mu_a + \mu_s(1 - g))^{-1}$

2,5,6 - see references in Supporting Information.

References

[1] van Norren D, Tiemeijer D. Spectral reflectance of the human eye. Vision Res. 1986;26:313-320.
[2] Hammer M, Roggan A, Schweitzer D, Muller G. Optical properties of ocular tissues - an in vitro study using the double-integrating-sphere technique and inverse Monte Carlo simulation. Phys. Med. Biol. 1995;40:964-978.
[3] van Blokland GJ, van Norren D. Intensity and polarization of light scattered at small angles from the human fovea. Vison Res. 1986;26:485-494.
[4] Hammer M, Schweitzer D. Quantitative reflection spectroscopy at the human ocular fundus. Phys. Med. Biol. 2002;47:179–191.
[5] Ferguson LR, Dominguez II JM, Balaiya S, Grover S, Chalam KV. Retinal Thickness Normative Data in Wild-Type Mice Using Customized Miniature SD-OCT. Plos One. *2013;8:e67265.*
[6] Sardar DK, Yust BG, Barrera FJ, Mimun LC, Tsin ATC. Optical absorption and scattering of bovine cornea, lens and retina in the visible region. Lasers Med. Sci. 2009;24:839-847.